# Adsorption and thermal stability of 2-mercaptobenzothiazole corrosion inhibitor on metallic and pre-oxidized Cu(111) model surfaces

Xiaocui Wu, Frédéric Wiame, Vincent Maurice, Philippe Marcus

# Adsorption and thermal stability of 2-mercaptobenzothiazole corrosion inhibitor on metallic and pre-oxidized Cu(111) model surfaces

Xiaocui WU, Frédéric Wiame*, Vincent Maurice, Philippe Marcus*

*Université PSL, CNRS - Chimie ParisTech, Institut de Recherche de ChimieParis, Groupe Physico-Chimie des Surfaces, 75005 Paris, France*

**Abstract**

2-mercaptobenzothiazole (2-MBT) is used for its corrosion inhibition properties. In this study, the adsorption of 2-MBT on metallic and pre-oxidized Cu(111) surfaces was investigated using Auger Electron Spectroscopy and Scanning Tunneling Microscopy. Growth and structure of molecular films adsorbed at ultra low pressure and room temperature on clean and pre-oxidized Cu(111) surfaces were characterized. On clean metallic Cu(111) surface, local triangular $(\sqrt{7} \times \sqrt{7})$R19.1° structures are formed at low exposures (3–4 L), which are assigned to the adsorption of atomic S resulting from partial decomposition of 2-MBT. At 10 L, a full non-ordered monolayer of 2-MBT is formed, and further exposure leads to the formation of a non-ordered multilayer. The thickness of the outermost 2-MBT layer is 1.3 Å, which suggests that the outermost molecules of the multilayer are lying flat. Oxidation of the copper surface prior to exposure to 2-MBT results in more compact and homogeneous molecular films. The initial 2D oxide is dissociated and replaced by 2-MBT. Thermal stability at different temperatures was studied on clean and pre-oxidized copper surfaces saturated with 2-MBT. A $(\sqrt{7} \times \sqrt{7})$R19.1° structure is observed in both cases for temperatures higher than 100°C, indicating the decomposition of 2-MBT and a copper surface covered with atomic S.

*Keywords:* 2-MBT, Corrosion inhibitor, Copper, STM, AES

*Corresponding authors

*Email addresses:* frederic.wiame@chimieparistech.psl.eu (Frédéric Wiame),

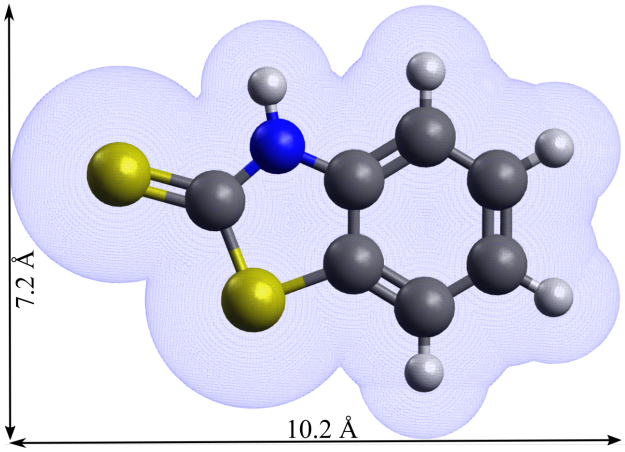


Figure 1: 2-MBT chemical structure (thione form) and associated molecular dimensions (the van der Waals surface is presented.)

## 1. Introduction

The corrosion of metals and alloys is an important issue in industrial applications with an annual global cost estimated to be about 3.4% of the global GDP (2013) [1]. In order to mitigate corrosion, inhibitors are widely used and developed. On copper, numerous studies [2–19] have been carried out for a better understanding of the surface interaction with corrosion inhibitors, as well as the inhibition mechanisms.

2-mercaptobenzothiazole (2-MBT) is one of the corrosion inhibitors used in industry besides benzotriazole (BTAH) [2–10]. Its chemical formula is $C_7H_5NS_2$, and it exists in two forms: the thione (NH) and the thiol (SH) forms. The former has C double bonded to S, and the latter C double bonded to endocyclic N with hydrogen bonded to S. It has been shown that 2-MBT is only in the thione form in gas phase [11]. The bond lengths and bond angles in the 2-MBT molecule have been determined [12], and by taking into consideration the van der Waals radii of different atoms, we can deduce its molecular dimensions, as shown in Fig. 1.

It has been shown that Cu reacts with 2-MBT in solution to form a complex which can protect it from corrosion [13, 14]. Woods et al. [15] claimed that 2-MBT is attached

philippe.marcus@chimieparistech.psl.eu (Philippe Marcus)

to the metal surface through interaction with the exocyclic sulfur, as well as the N atom [4, 16, 17], but not by the endocyclic S atom. It was also suggested that 2-MBT adsorbs flat on Ag in the thiol form, while it adsorbs with molecular plane perpendicular on Au in thione form [18]. 2-MBT can also protect aluminium alloy from corrosion by forming a thin organic layer on the substrate surface [20]. Besides the molecular deposition in solution, the adsorption of BTAH on Cu(111) surface has been investigated by gas evaporation under ultra-high vacuum (UHV) and analyzed by scanning tunneling microscopy (STM) [19]. A chemisorbed monolayer was formed firstly, followed by physisorbed multilayer which were less stable and desorb at around 100°C.

In this work, we studied the interaction of 2-MBT with a single crystalline Cu(111) surface using Auger Electron Spectroscopy (AES) and STM. It allows us to determine the adsorption process and address the adsorbed molecular structure at nanometric and atomic scales. The influence of surface pre-oxidation and the effect of temperature were also investigated. This study brings new insight into the inhibition mechanism of 2-MBT on copper, which contributes to the knowledge-based development of more efficient corrosion inhibitors for the corrosion protection of copper and its alloys.

## 2. Experimental

A Cu(111) single crystal of high purity (99.999%) was used. The surface was mechanically polished down to 0.25 $\mu$m (diamond paste), and then electro-polished in 60 wt% $H_3PO_4$ solution at 1.4 V during 5 min before introduction into the UHV system, where it was further prepared by cycles of ion sputtering ($P_{\mathrm{Ar}} = 1 \times 10^{-5}$ mbar, 600 V, 20 mA, 30 min) and annealing (600°C, 30 min) in order to obtain a clean and well-structured surface. The base pressure of the UHV system is $10^{-10}$ mbar, and it is equipped with STM (Omicron, STM1 with SCALA system), AES (Omicron model CMA-100) and Low Energy Electron Diffraction (LEED, Riber, OPD-304). The surface was systematically checked by AES, LEED and STM until no contamination and a good surface organization were observed, characterized by a sharp (1×1) LEED pattern and a topography with large and flat terraces as verified by STM.

The 2-MBT molecule used was 99% pure (Sigma-Aldrich). It is a yellow powder at room temperature. The 2-MBT powder was placed in a vacuum sealed glass connected directly to a reactor attached to the UHV system. The pressure of 2-MBT in the reactor was $2 \times 10^{-9}$ mbar at room temperature. The sample was kept at room temperature during the deposition process. In order to investigate the influence of pre-oxidation on the adsorption of 2-MBT, oxidation of the copper surface was performed by introducing oxygen gas in the chamber through a leak valve ($P_{O_2} = 5 \times 10^{-6}$ mbar) until saturation. In these conditions, a 2D surface oxide is formed [21–23]. After 2-MBT depositions on clean and pre-oxidized copper surfaces, the growth kinetics was followed by AES, and the surface structures were characterized by STM.

The STM measurements were performed at room temperature and in constant current mode. Image processing was carried out using WSxM software (5.0 Develop 9.1) [24]. No filtering was applied except when mentioned. All images were corrected by plane subtraction.

## 3. Results and discussion

### *3.1. 2-MBT adsorption on metallic Cu(111) surface*

A clean oxide-free and organized copper surface was prepared under UHV, then the sample was exposed to 2-MBT at ultra low pressure ($2 \times 10^{-9}$ mbar) and room temperature and analyzed by AES. Fig. 2 shows the change in the peak-to-peak height ratios of S (151 eV), C (271 eV) and N (380 eV) to Cu (920 eV) signals as a function of exposure to 2-MBT. The adsorption of 2-MBT is initially characterized by fast increase of the S, C and N signals with increasing exposure, indicating the deposition of 2-MBT on the sample surface, and then a decrease in the adsorption rate until saturation of the measured signals after an exposure of about 100 L. The limit values for $h_S/h_{Cu}$, $h_C/h_{Cu}$ and $h_N/h_{Cu}$ are 2.6 ± 0.3, 1.2 ± 0.1 and 0.19 ± 0.02, respectively.

In order to verify that the increase of the S, C and N signals corresponds to the adsorption of 2-MBT, their relative ratios are corrected using the relative sensitivities $S_x$ of the Auger transitions. The results are shown in Fig. 3. The corrected N to C ratio calculated after

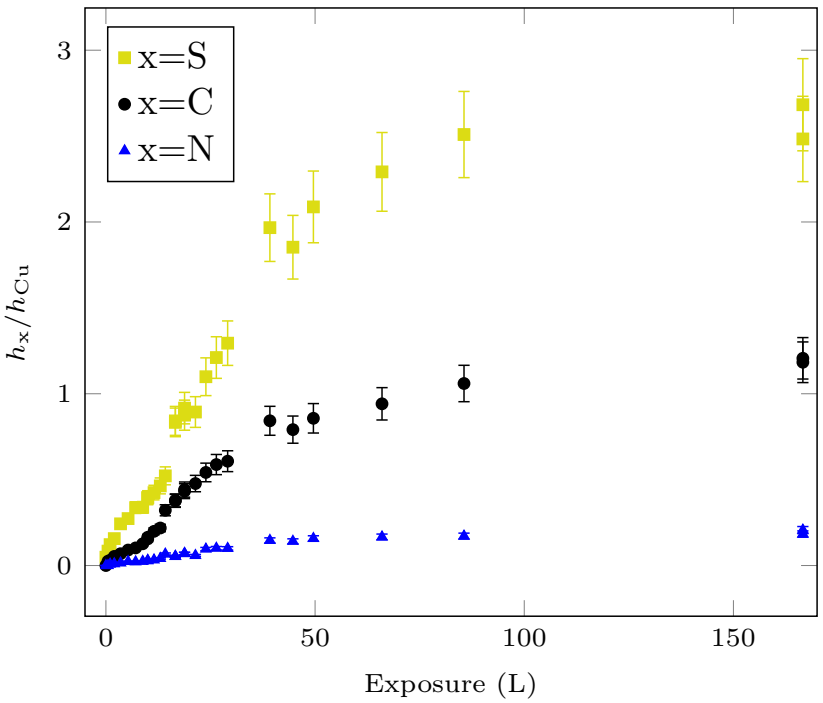


Figure 2: Growth kinetics of 2-MBT on Cu(111) at room temperature. Change in the AES peak-to-peak height ratios $h_S/h_{Cu}$, $h_C/h_{Cu}$ and $h_N/h_{Cu}$ as a function of 2-MBT exposure at $2\times10^{-9}$ mbar.

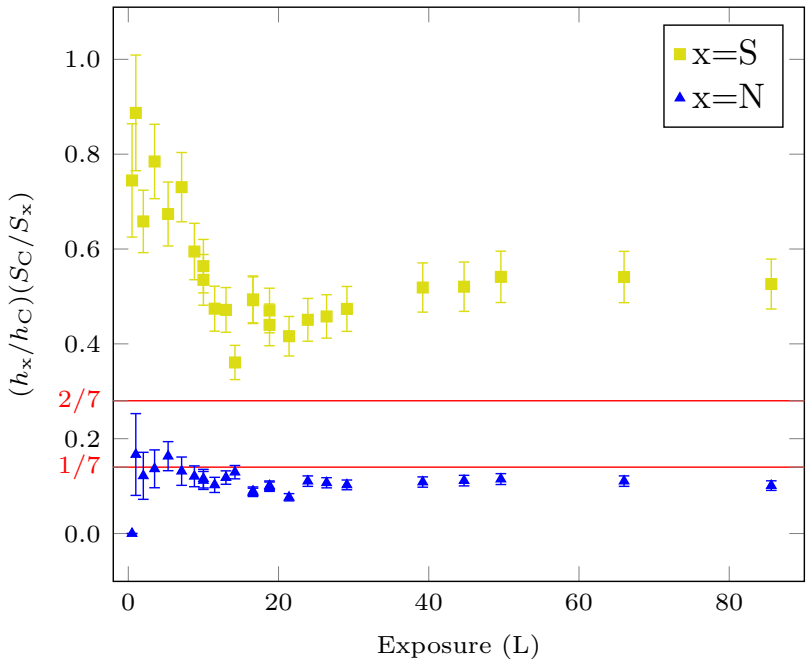


Figure 3: Evolution of S and N to C atomic ratios as measured by AES with 2-MBT exposure at ultra low pressure and RT.

different exposures is close to the theoretical (molecule stoichiometry) value (1/7), deduced from the number of N and C atoms in the molecule, indicating the adsorption of 2-MBT on Cu(111). However, the S to C ratio first decreases and then increases slightly after about 10 L until reaching its saturation value. This seems to indicate that there is a transition in the growth mode of 2-MBT at about 10 L, also suggested in Fig. 2 by the change in slope. Another point to notice is that the ratio between S and C at stationary regime is almost 2 times the theoretical value (2/7).

In order to explain this excess of S, STM measurements were carried out at different exposures to characterize the surface structure.

Low exposure, i.e. 4 L, is characterized by the formation of ordered local structures along the step edges and on the terraces, as shown in Fig. 4a. These local structures are triangles having variable dimension (side length of 2–3 nm). The triangles are either isolated or aggregated. Similar triangles have been observed for atomic S adsorbed on the Cu(111)

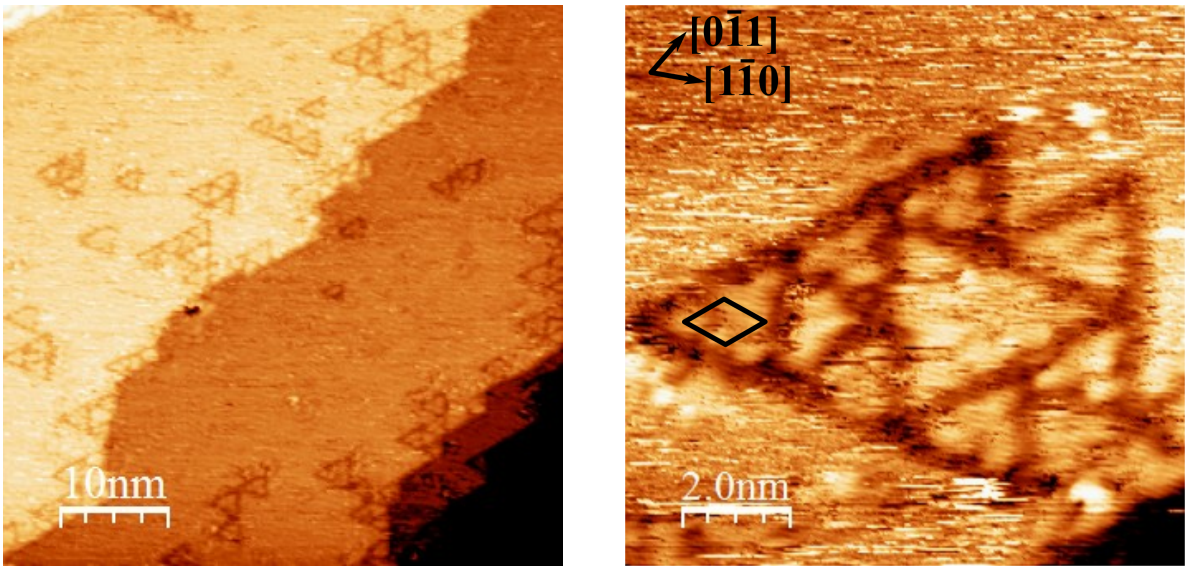


(a) (b)

Figure 4: STM images for 4 L (exposure) of 2-MBT on Cu(111) (a) 50 nm × 50 nm, $V = -1.0$ V, $I = 1.0$ nA; (b) 10 nm × 10 nm, $V = -1.0$ V, $I = 0.5$ nA.

surface [25, 26], which seems to indicate the adsorption of S atoms on the copper surface in the present case. However, in the case of S/Cu(111), due to the high mobility of atomic S at low coverage, the triangles were mainly at the step edges. Here, adsorbed molecules on Cu(111) may play the role of a barrier, thus preventing the displacement of S, which could explain the formation of triangles on the terraces and not only at the step edges.

A higher resolution image of these triangles is presented in Fig. 4b. Substrate crystallographic directions, derived from atomic resolution STM images and LEED pattern obtained on pristine Cu(111) surface, are shown. An ordered local structure can be observed inside the triangles with the presence of three or six protrusions depending on the size of triangles. The lattice unit cell is shown by the black rhombus. The distance between protrusions in different directions and from different STM images was measured to be $0.67 \pm 0.02$ nm, thus we identified the lattice as a $(\sqrt{7} \times \sqrt{7})$R19.1° structure, which is similar to that obtained for the S/Cu(111) system at saturation [27, 28]. This suggests the local adsorption of atomic S on copper, and a partial decomposition of 2-MBT when interacting with the clean, metallic Cu(111) surface, which explains the excess of S observed in Fig. 3. By counting the

number of protrusions inside the triangles of different sizes in Fig. 4a, we estimate their density on the surface to be $\sim 2\times10^{13}$ cm$^{-2}$. Given that the atomic density of copper atoms on Cu(111) surface is $1.78\times10^{15}$ cm$^{-2}$, we estimate a surface coverage (ratio between the density of protrusion and the atomic density of the substrate) of $\sim 1\%$. A well-organized $(\sqrt{7}\times\sqrt{7})$R19.1° surface gives a coverage of 14%, assuming one adsorbate per unit cell.

Further exposure of the sample to 2-MBT up to 10 L (Fig. 5) preserves the surface topography. Small darker local structures are observed on the terraces, as indicated by the white triangle. These structures are similar in size and orientation to the triangular structures observed on Cu(111) at 4 L, and can be assigned to the adsorption of atomic S. The apparent height difference between these structures and the terraces nearby is about 0.7 Å, which is smaller than that between two successive Cu(111) planes, i.e. 2.0 Å. This seems to indicate the formation of a quasi-complete layer of molecules which lie almost flat on the sample surface by referring to the size of the molecule, with the adsorption of both atomic S resulting from molecular partial decomposition and 2-MBT in its molecular form. The results are in good agreement with AES measurements (Fig. 3) showing a change of slope at 10 L and an excess of S. No local ordering was evidenced by Fast Fourier Transform (FFT) of the images.

At higher exposure, 2-MBT continues to adsorb on Cu, and finally more than one molecular layer is formed. The surface obtained after an exposure of 1300 L (Fig. 6a) is rougher than that obtained for 10 L. One can still see different terraces but the contrast between different zones on terraces is increased (Fig. 6b). This corresponds to difference in height, i.e. the thickness, due to adsorption of the last molecular layer. This contrast also indicates that the last molecular layer is incomplete. We can plot the height distribution of a terrace, as shown by the height histogram (Fig. 6c), obtained from Fig. 6b with a bin size of 5 pm. Fitting of the histogram with gaussian distributions gives a layer thickness of 1.3 Å and a surface covered fraction of 55% for the last molecular layer. Taking into account the molecular dimensions of 2-MBT, this indicates that the 2-MBT in the last molecular layer adsorbs with its plane almost parallel to sample surface. FFT did not reveal any ordered local structure.

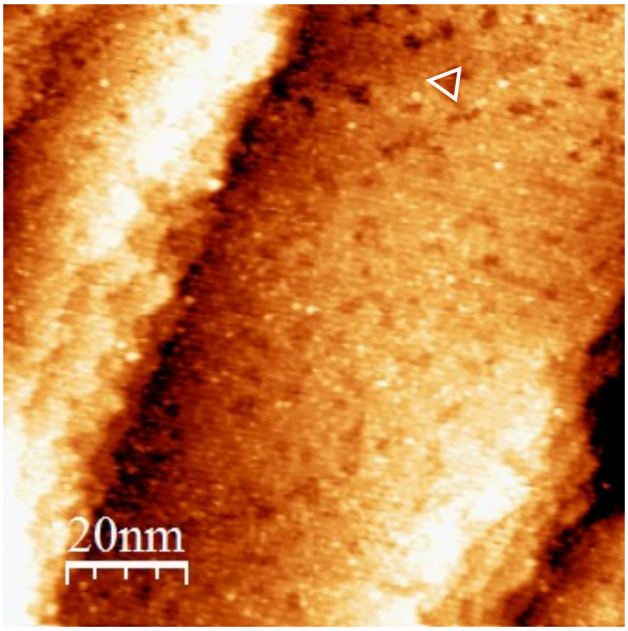


Figure 5: STM image for 10 L (exposure) of 2-MBT on Cu(111) (100 nm × 100 nm, $V = -2.0$ V, $I = 0.2$ nA).

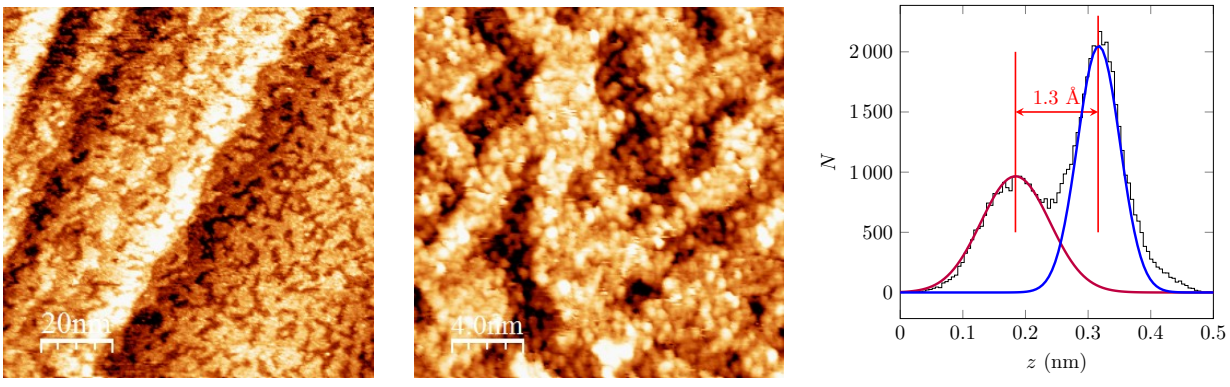


(a) (b) (c)

Figure 6: STM images for 1300 L (exposure) of 2-MBT on Cu(111) (a) 100 nm × 100 nm, $V = 1.0$ V, $I = 0.2$ nA; (b) 20 nm × 20 nm, $V = 1.0$ V, $I = 0.3$ nA; (c) Height histogram of image (b).

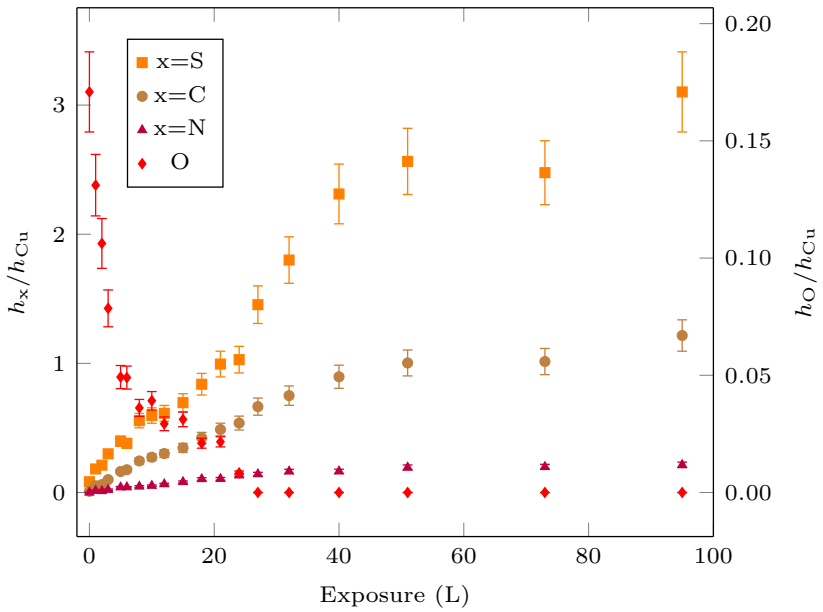


Figure 7: Growth kinetics of 2-MBT on pre-oxidized Cu(111) at room temperature. Changes in Auger peak-to-peak height ratios as a function of 2-MBT exposure at $2{\times}10^{-9}$ mbar.

### *3.2. 2-MBT adsorption on pre-oxidized Cu(111) surface*

In order to investigate the influence of pre-oxidation on the adsorption of 2-MBT, the Cu(111) surface covered previously with a 2D surface oxide was prepared by exposing the clean surface to gaseous oxygen ($P_{O_2} = 5 \times 10^{-6}$ mbar) during 15 min at room temperature [22].

Fig. 7 shows the evolution of the peak-to-peak height ratios of S (151 eV), C (271 eV) and N (380 eV) to Cu (920 eV) Auger signals with 2-MBT exposure at room temperature. Similarly to Fig. 2, a first region with rapid increase of the S, C and N signals is observed, indicating the growth of the 2-MBT layer on the pre-oxidized copper surface, followed by a saturation regime, characterized by the plateau in the S, C and N signals. At saturation, the value of $h_S/h_{Cu}$ ($\sim 2.8 \pm 0.3$) is similar to that obtained without pre-oxidation.

It is important to notice that the growth of the 2-MBT layer is accompanied by a continuous decrease of the $h_O/h_{Cu}$ signal from $0.17 \pm 0.02$ to zero. Oxygen initially present on the sample surface is thus substituted by 2-MBT and completely desorbs at 2-MBT exposure of about 25 L at room temperature. The substitution of oxygen by sulfur has also

been observed for $H_2S$ exposure on pre-oxidized Cu(111) surface [29].

The STM image of the pre-oxidized surface (Fig. 8a) confirms the formation of a flat bi-dimensional copper oxide covering the atomically flat substrate terraces, with a reconstruction of the step edges. Moreover, local defects exist on the terraces, and they appear darker than the terraces, with a difference in height of about 2 Å, corresponding to the height of one atomic step of Cu(111).

The pre-oxidized surface was then exposed to 2-MBT, and no obvious change of the surface topography is observed, as shown in Fig. 8b and Fig. 8c (high frequency noise has been filtered in Fig. 8c). The terraces remain flat and homogeneous after exposure to 2-MBT, and the step edges keep a similar form as before exposure. Local defects are always present on the terraces with similar height compared to that measured on the pre-oxidized copper surface before exposure. No ordered local structure was observed.

Compared to the multilayer-covered surface obtained by exposing clean, metallic Cu(111) to 2-MBT (Fig. 5 and Fig. 6), the terrace topography is more compact and uniform on the pre-oxidized surface, indicating that the last molecular layer is almost complete. So we can conclude that pre-oxidation of copper prior to exposure can effectively change the morphology of the adsorbed 2-MBT multilayer. It appears likely that the Cu atoms released by the dissociation of the 2D copper oxide favor the formation of a more homogeneous and compact multilayer of 2-MBT.

### *3.3. Thermal stability of 2-MBT layers*

In order to test the stability of the adsorbed molecular layer, annealing at different temperatures was carried out for multilayer deposited on metallic and pre-oxidized Cu(111) surfaces, which were then characterized by STM and LEED after annealing.

Fig. 9 shows that the topography of clean Cu(111) surface saturated with 2-MBT changes after annealing at 160°C. Reorganization of the steps can be observed, with the formation of straight and parallel step edges. The step edges become aligned along the principal direction of the surface layer, as can be seen from the comparison of Fig. 9 and Fig. 10a. Moreover, bright spots can be evidenced on the terraces, with size of 1–2 nm, and height of about 1

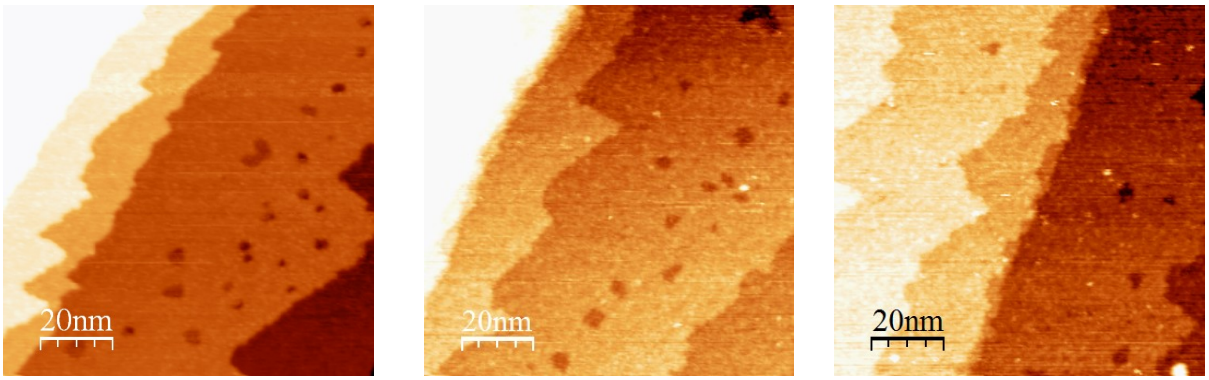


(a) (b) (c)

Figure 8: STM images of pre-oxidized Cu(111) surface (a) before exposure to 2-MBT (100 nm × 100 nm, $V = 1.0$ V, $I = 0.2$ nA); (b) after 21 L of 2-MBT (100 nm × 100 nm, $V = 1.0$ V, $I = 0.6$ nA); (c) after 40 L of 2-MBT (100 nm × 100 nm, $V = 0.7$ mV, $I = 0.3$ nA).

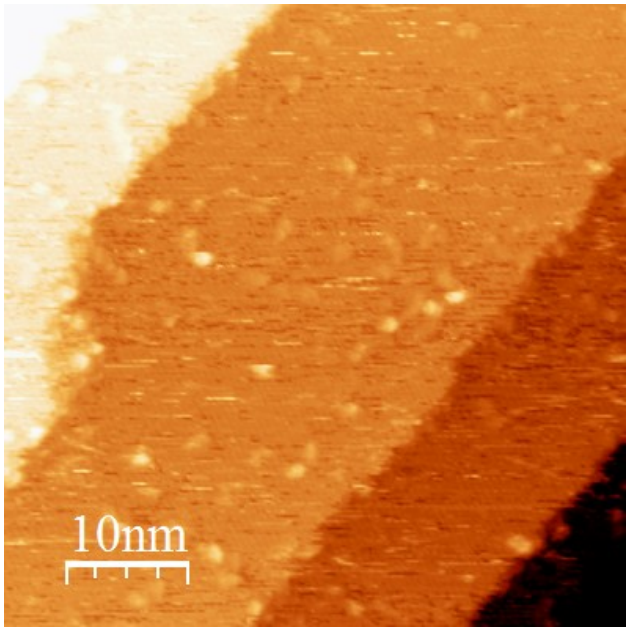


Figure 9: STM image of clean Cu(111) surface exposed to MBT (saturation) after annealing at 160°C (50 nm × 50 nm, $V = -1.0$ V, $I = 0.2$ nA).

Å. They may be assigned to the decomposition products after annealing.

If we zoom in on a terrace (Fig. 10a), we can see that the $(\sqrt{7} \times \sqrt{7})$R19.1° structure is formed, also confirmed by FFT (Fig. 10b). This is the characteristic structure obtained when Cu(111) surface is exposed to atomic S until saturation [27, 28]. The annealing tests were performed at different temperatures, and the $(\sqrt{7} \times \sqrt{7})$R19.1° structure was observed once the sample was heated above 100°C, also confirmed by LEED as shown in Fig. 10c. Two overlapped mirror domains are observed by LEED, as indicated in Fig. 10d. Mirror domains are also observed in STM images obtained from different area on the surface. Taking into account the possible elements present on the surface (S, C, N, O) measured by AES, we can deduce that 2-MBT dissociates when heated to temperatures above 100°C, and atomic S remains adsorbed on the copper surface. The same phenomenon is observed on pre-oxidized Cu(111) surface saturated with 2-MBT after annealing at temperatures superior to 100°C, indicating the decomposition and partial desorption of molecular layers adsorbed on pre-oxidized Cu(111) surface.

## 4. Conclusion

In this study, the morphology and structure of 2-MBT layers adsorbed on metallic and pre-oxidized Cu(111) surfaces at room temperature and their thermal stability were investigated by AES and STM in order to bring nanometric and atomic scale insight on the interaction of the molecule with copper, which is of paramount importance for its corrosion inhibition properties. On clean, metallic Cu(111) surface, local $(\sqrt{7} \times \sqrt{7})$R19.1° ordered triangular structures, typical of atomic S adsorption on Cu(111), are observed at low exposures, suggesting a partial decomposition of 2-MBT and adsorption of atomic S on Cu(111). 2-MBT forms a monolayer of adsorbed molecules at an exposure of about 10 L which is almost lying flat on copper. A non ordered 2-MBT multilayer is formed at higher exposure, with an incomplete outermost molecular layer of thickness of 1.3 Å and of surface covered fraction of 55%. Taking into account the dimension of 2-MBT, we can conclude that the outermost molecules adsorb flat on the surface.

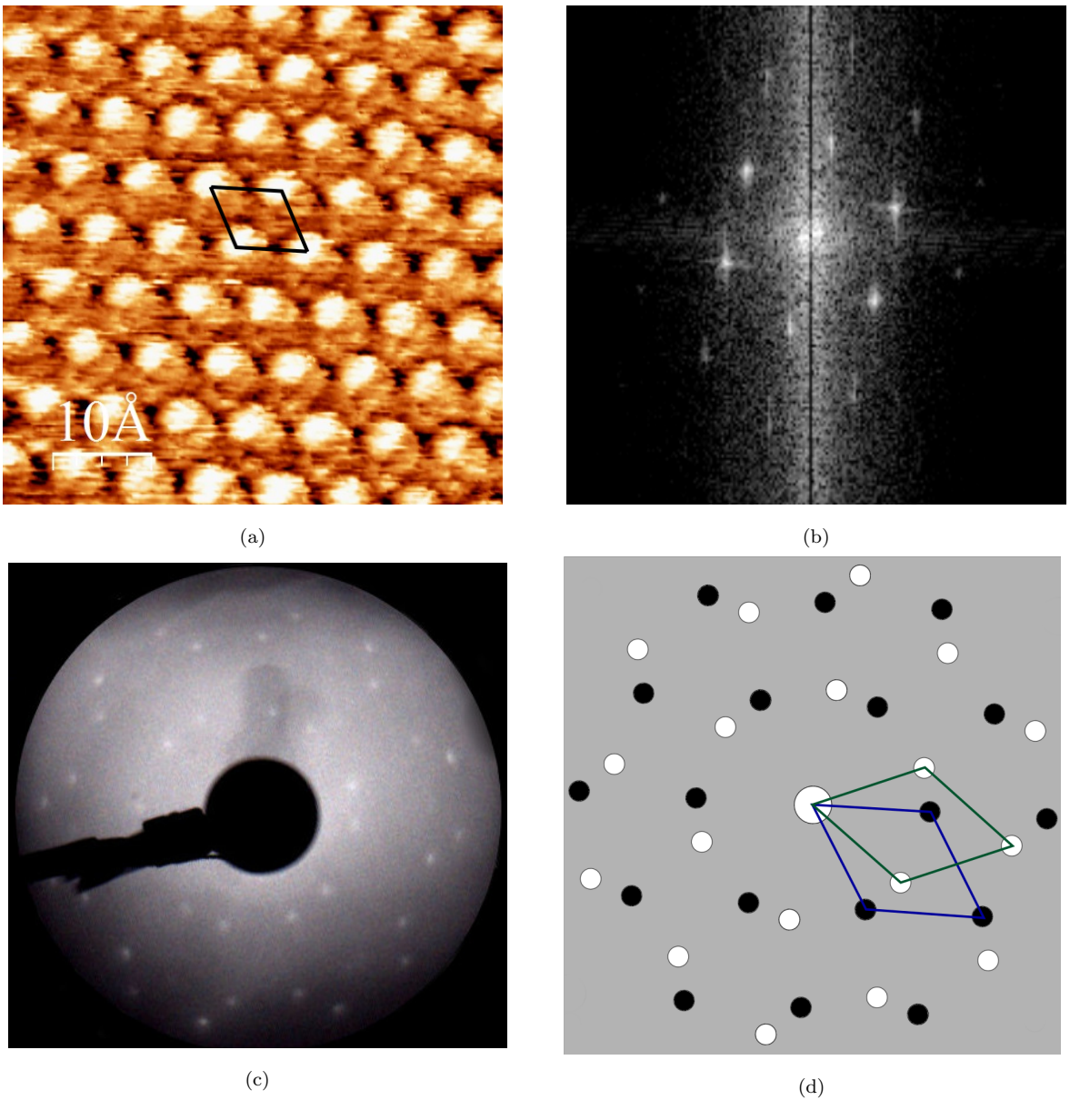


Figure 10: Clean Cu(111) surface exposed to MBT (saturation) after annealing (a) at 160°C observed by STM (5 nm × 5 nm, $V = -0.1$ V, $I = 2.5$ nA); (b) FFT of (a); (c) at 200°C observed by LEED (Ep = 50 eV); (d) schematics with the unit cells associated with the two variants of the superstructure.

When Cu(111) is pre-oxidized and covered by a 2D surface oxide layer, the sample surface remains flat and homogeneous after 2-MBT dosing, and the last molecular layer formed is complete. The 2D oxide layer is replaced by 2-MBT and the presence of Cu atoms from the dissociated 2D oxide promotes a homogeneous morphology of the molecular layer with a local structure that remains non ordered.

The stability of the molecular multilayer adsorbed on clean and pre-oxidized Cu(111) surfaces was investigated by annealing. In both cases, when the sample was heated above 100°C, the step edges are reorganized, and the surface is completely covered by a $(\sqrt{7} \times \sqrt{7})$R19.1° structure, typical of S/Cu(111) system at saturation, indicating the decomposition and partial desorption of 2-MBT and the adsorption of S atoms on the sample surface.

## 5. Acknowledgments

This project has received funding from the European Research Council (ERC) under the European Union's Horizon 2020 research and innovation program (ERC Advanced Grant CIMNAS no. 741123).

## References

[1] http://impact.nace.org/economic-impact.aspx.

[2] M. M. Antonijević, M. B. Petrović, Copper corrosion inhibitors. A review, International journal of electrochemical science 3 (1) (2008) 1–28.

[3] L. P. Kazansky, Y. E. Pronin, I. A. Arkhipushkin, XPS study of adsorption of 2-mercaptobenzothiazole on a brass surface, Corrosion Science 89 (2014) 21–29.

[4] Y.-H. Chen, A. Erbe, The multiple roles of an organic corrosion inhibitor on copper investigated by a combination of electrochemistry-coupled optical in situ spectroscopies, Corrosion Science 145 (2018) 232–238.

[5] T. Yoshida, K. Yamasaki, S. Sawada, An X-ray photoelectron spectroscopic study of 2-mercaptobenzothiazole metal complexes, Bulletin of the Chemical Society of Japan 52 (10) (1979) 2908–2912.

[6] M. B. Petrović Mihajlović, M. M. Antonijević, Copper corrosion inhibitors. Period 2008-2014. A review, International journal of electrochemical science 10 (2015) 1027–1053.

[7] F. M. Al Kharafi, N. A. Al-Awadi, I. M. Ghayad, R. M. Abdullah, M. R. Ibrahim, Novel technique for the application of azole corrosion inhibitors on copper surface, Materials transactions 51 (9) (2010) 1671–1676.

[8] G. Gece, Drugs: A review of promising novel corrosion inhibitors, Corrosion Science 53 (12) (2011) 3873–3898.

[9] A. Fateh, M. Aliofkhazraei, A. R. Rezvanian, Review of corrosive environments for copper and its corrosion inhibitors, Arabian Journal of Chemistry In press (2017) http://dx.doi.org/10.1016/j.arabjc.2017.05.021.

[10] M. M. Antonijević, S. M. Milić, M. B. Petrović, Films formed on copper surface in chloride media in the presence of azoles, Corrosion Science 51 (2009) 1228–1237.

[11] G. Contini, V. D. Castro, S. Stranges, R. Richter, M. Alagia, Gas-phase photoemission study of 2-mercaptobenzothiazole, The Journal of Physical Chemistry A 106 (2002) 2833–2837.

[12] J. P. Chesick, J. Donohue, The molecular and crystal structure of 2-mercaptobenzothiazole, Acta Crystallographica Section B B27 (1971) 1441–1444.

[13] E. M. M. Sutter, F. Ammeloot, M. J. Pouet, C. Fiaud, R. Couffignal, Heterocyclic compounds used as corrosion inhibitors: correlation between 13C and 1H NMR spectroscopy and inhibition efficiency, Corrosion Science 41 (1999) 105–115.

[14] R. Subramanian, V. Lakshminarayanan, Effect of adsorption of some azoles on copper passivation in alkaline medium, Corrosion Science 44 (2002) 535–554.

[15] R. Woods, G. A. Hope, K. Watling, A SERS spectroelectrochemical investigation of the interaction of 2-mercaptobenzothiazole with copper, silver and gold surfaces, Journal of Applied Electrochemistry 30 (2000) 1209–1222.

[16] M. Finšgar, D. K. Merl, An electrochemical, long-term immersion, and XPS study of 2-mercaptobenzothiazole as a copper corrosion inhibitor in chloride solution, Corrosion Science 83 (2014) 164–175.

[17] L. P. Kazansky, I. A. Selyaninov, Y. I. Kuznetsov, Adsorption of 2-mercaptobenzothiazole on copper surface from phosphate solutions, Applied Surface Science 258 (2010) 6807–6813.

[18] N. Sandhyarani, G. Skanth, S. Berchmans, V. Yegnaraman, T. Pradeep, A combined surface-enhanced Raman–X-Ray photoelectron spectroscopic study of 2-mercaptobenzothiazole monolayers on polycrystalline Au and Ag films, Journal of Colloid and Interface Science 209 (1999) 154–161.

[19] F. Grillo, D. Tee, S. Francis, H. Früchtl, N. Richardson, Passivation of copper: Benzotriazole films on Cu(111), The Journal of Physical Chemistry C 118 (16) (2014) 8667–8675.

[20] M. Zheludkevich, K. Yasakau, S. Poznyak, M. Ferreira, Triazole and thiazole derivatives as corrosion inhibitors for AA2024 aluminium alloy, Corrosion Science 47 (12) (2005) 3368–3383.

[21] T. Matsumoto, R. Bennett, P. Stone, T. Yamada, K. Domen, M. Bowker, Scanning tunneling microscopy studies of oxygen adsorption on Cu(111), Surface Science 471 (2001) 225–245.

[22] F. Wiame, V. Maurice, P. Marcus, Initial stages of oxidation of Cu(111), Surface Science 601 (2007) 1193–1204.

[23] R.W.Judd, P. Hollins, J. Pritchard, The interaction of oxygen with Cu(111): Adsorption, incorporation and reconstruction, Surface Science 171 (1986) 643–653.

[24] I. Horcas, R. Fernández, J. M. Gómez-Rodríguez, J. Colchero, J. Gómez-Herrero, A. M. Baro, Wsxm: A software for scanning probe microscopy and a tool for nanotechnology, Review of Scientific Instruments 78 (2007) 013705.

[25] E. Wahlström, I. Ekvall, H. Olin, S.-A. Lindgren, L. Walldén, Observation of ordered structures for S/Cu(111) at low temperature and coverage, Physical Review B 60 (15) (1999) 10699–10702.

[26] E. Wahlström, I. Ekvall, T. Kihlgren, H. Olin, S.-A. Lindgren, L. Walldén, Low-temperature structure of S/Cu(111), Physical Review B 64 (2001) 155406.

[27] L. Ruan, I. Stensgaard, F. Besenbacher, E. Laegsgaard, A scanning tunneling microscopy study of the interaction of S with the Cu(111) surface, Ultramicroscopy 42-44 (1992) 498–504.

[28] C. T. Campbell, B. E. Koel, $H_2S$/Cu(111): A model study of sulfur poisoning of water-gas shift catalysts, Surface Science 183 (1-2) (1987) 100–112.

[29] F. Wiame, V. Maurice, P. Marcus, Reactivity to sulphur of clean and pre-oxidised Cu(111) surfaces, Surface science 600 (18) (2006) 3540–3543.